



Cr-Doped $\text{Li}_2\text{ZnTi}_3\text{O}_8$ as a High Performance Anode Material for Lithium-Ion Batteries

Xianguang Zeng^{1,2*}, Jing Peng¹, Huafeng Zhu^{3*}, Yong Gong¹ and Xi Huang¹

¹ Institute of Material, Sichuan University of Science and Engineering, Zigong, China, ² Material Corrosion and Protection Key Laboratory of Sichuan Province, Zigong, China, ³ Langxingda Technology Co, Ltd., Zigong, China

$\text{Li}_2\text{ZnTi}_{2.9}\text{Cr}_{0.1}\text{O}_8$ and $\text{Li}_2\text{ZnTi}_3\text{O}_8$ were synthesized by the liquid phase method and then studied comparatively using X-ray diffraction (XRD), scanning electron microscopy (SEM), X-ray photoelectron spectroscopy (XPS), galvanostatic charge–discharge testing, cyclic stability testing, rate performance testing, and electrochemical impedance spectroscopy (EIS). The results showed that Cr-doped $\text{Li}_2\text{ZnTi}_3\text{O}_8$ exhibited much improved cycle performance and rate performance compared with $\text{Li}_2\text{ZnTi}_3\text{O}_8$. $\text{Li}_2\text{ZnTi}_{2.9}\text{Cr}_{0.1}\text{O}_8$ exhibited a discharge ability of 156.7 and 107.5 mA h g^{-1} at current densities of 2 and 5 A g^{-1} , respectively. In addition, even at a current density of 1 A g^{-1} , a reversible capacity of 162.2 mA h g^{-1} was maintained after 200 cycles. The improved electrochemical properties of $\text{Li}_2\text{ZnTi}_{2.9}\text{Cr}_{0.1}\text{O}_8$ are due to its increased electrical conductivity.

Keywords: lithium ion battery, $\text{Li}_2\text{ZnTi}_3\text{O}_8$, Cr doping, anode material, $\text{Li}_2\text{ZnTi}_{2.9}\text{Cr}_{0.1}\text{O}_8$

OPEN ACCESS

Edited by:

Bin Huang,
Guilin University of Technology, China

Reviewed by:

Ting-Feng Yi,
Northeastern University at
Qinhuangdao, China
Hongwei Mi,
Shenzhen University, China

*Correspondence:

Xianguang Zeng
hnxzg1979@126.com
Huafeng Zhu
53068972@qq.com

Specialty section:

This article was submitted to
Electrochemistry,
a section of the journal
Frontiers in Chemistry

Received: 29 August 2020

Accepted: 30 September 2020

Published: 28 January 2021

Citation:

Zeng X, Peng J, Zhu H, Gong Y and
Huang X (2021) Cr-Doped $\text{Li}_2\text{ZnTi}_3\text{O}_8$
as a High Performance Anode
Material for Lithium-Ion Batteries.
Front. Chem. 8:600204.
doi: 10.3389/fchem.2020.600204

INTRODUCTION

Lithium-ion batteries (LIBs) are a new type of rechargeable batteries that are characterized by high specific capacities and specific energies, small volumes, long life cycles, low cost, low energy consumption, low self-discharge efficiencies, small internal resistance, and high working voltages (Yoshio, 2001; Junmin et al., 2005; Dong-il and Han, 2006; Wang M. X. et al., 2019; Wang S. et al., 2019; Huang et al., 2020; Wang et al., 2020; Yi et al., 2020a), and they have wide applications, including in mobile phones, laptops, cameras, digital cameras, electric automobiles, energy storage, aerospace, and space exploration (Tarascon and Armand, 2001; Xiao et al., 2018, 2019; An et al., 2019; Hong et al., 2019). The selection of suitable anode materials for LIBs is extremely important for the performance of these batteries to have excellent life cycles and charge/discharge rate characteristics.

Recently, there have been numerous studies of anode materials, including LiTi_2O_4 , $\text{Li}_2\text{Ti}_3\text{O}_7$, $\text{Li}_2\text{Ti}_6\text{O}_{13}$, $\text{Li}_4\text{Ti}_5\text{O}_{12}$, $\text{Na}_2\text{Li}_2\text{Ti}_6\text{O}_{14}$, TiNb_2O_7 , and $\text{Li}_2\text{ZnTi}_3\text{O}_8$ (Tang et al., 2014a; Chen B. K. et al., 2015; Li G. H. et al., 2016; Liu et al., 2016; Li Z. F. et al., 2016; Yi et al., 2020b). $\text{Li}_2\text{ZnTi}_3\text{O}_8$ with the cubic spinel structure has been considered as a promising material because of its lack of toxicity, low cost, relatively high theoretical capacity of 227 mA h g^{-1} , and its low discharge voltage plateau of ~ 0.5 V (vs. Li/Li^+) (Jović et al., 2009; Chen B. K. et al., 2015; Chen W. et al., 2015). However, compared with other anode materials, $\text{Li}_2\text{ZnTi}_3\text{O}_8$ suffers from low electronic conductivity and an even worse rate performance, which means that its performance in practice is lower than the theoretical value (Tang and Tang, 2014; Chen B. K. et al., 2015). Hence, by increasing its electronic conductivity, its use can be extended to a wider range of applications.

Until now, this problem has been solved by applying a synthesized coating containing conductive species, nano-sized particles, and doping ions (Shenouda and Murali, 2008; Qi et al., 2009; Tian et al., 2010; Lin et al., 2011, 2013; Yu et al., 2011; Zhang et al., 2011; Bai et al., 2012; Jhan and Duh, 2012; Wu et al., 2013; Xu et al., 2013; Mani et al., 2014; Tang et al., 2014a; Yi et al., 2020c). As is widely known, by using a synthesized coating with conductive species on $\text{Li}_2\text{ZnTi}_3\text{O}_8$, the transportation of electrons can be improved while decreasing the particle size, which further accelerates ionic transportation. Moreover, it has been shown that doping ions into the material can increase its internal electronic conductivity (Lee et al., 2010; Fang et al., 2013; Lin et al., 2014). According to previous studies, the introduction of Al (Tang et al., 2014b), Ag (Tang et al., 2014a), Mo (Wang M. X. et al., 2019), and Ti (III) (Chen et al., 2018) to $\text{Li}_2\text{ZnTi}_3\text{O}_8$ greatly improved the electrochemical properties of these materials. For example, Tang et al. (2014b) partially replaced Ti with Al, and the resulting $\text{Li}_2\text{ZnTi}_{2.9}\text{Al}_{0.1}\text{O}_8$ composite showed a given capacity of $223.1 \text{ mA h g}^{-1}$ at 0.1 A g^{-1} (Tang et al., 2014b). Wang M. X. et al. (2019) improved the electronic conductivity of the $\text{Li}_2\text{ZnTi}_3\text{O}_8$ compound by introducing Mo, and $\text{Li}_2\text{Zn}_{0.93}\text{Mo}_{0.07}\text{Ti}_3\text{O}_8$ @graphene showed a high cycle capacity at high current densities of 5 A g^{-1} , with a power rating of 153 mA h g^{-1} still being delivered on the 200th cycle (Wang M. X. et al., 2019). Recently, researchers have paid close attention to the use of Cr doping, which, according to one study (Ruan et al., 2017), can further enhance the electronic conductivity. Pan et al. (2018) have successfully prepared Cr-doped $\gamma\text{-Fe}_2\text{O}_3/\text{rGO}$ cathode material by microwave method. The as-obtained 4.0 at% Cr-doped $\gamma\text{-Fe}_2\text{O}_3/\text{rGO}$ sample exhibits the capacity of $1,060 \text{ mAh g}^{-1}$ after 100 cycles at 100 mA g^{-1} . Liu et al. (2018) have prepared $\text{Fe}_{1.95}\text{Cr}_{0.05}\text{F}_5\cdot\text{H}_2\text{O}$ material, which retains a discharge capacity of 171 mAh g^{-1} after 100 cycles at 0.1 C ($1 \text{ C} = 200 \text{ mAh g}^{-1}$). Feng et al. (2009) have successfully synthesis Cr- LiV_3O_8 cathode material, and it showed an excellent electrochemical performance, with the retention of 94.4% after 100 cycles. To the best of our knowledge, the introduction of Cr^{3+} -doped ions into $\text{Li}_2\text{ZnTi}_3\text{O}_8$ has not yet been reported. In this paper, we describe the improvement in electrochemical performance of $\text{Li}_2\text{ZnTi}_3\text{O}_8$ anode material as a result of Cr doping.

MATERIALS AND METHODS

$\text{Li}_2\text{ZnTi}_{2.9}\text{Cr}_{0.1}\text{O}_8$ was prepared by the liquid phase method. Stoichiometric amounts of TiO_2 , $(\text{CH}_3\text{COO})\text{Li}$, $(\text{CH}_3\text{COO})_2\text{Zn}$, and $\text{Cr}(\text{NO}_3)_3$ were mixed with anhydrous ethanol as solvent. The mixture was dried at 80°C for 2 h and then roasted in a muffle furnace at 700°C for 10 h to obtain the final $\text{Li}_2\text{ZnTi}_{2.9}\text{Cr}_{0.1}\text{O}_8$ compound. For comparison, $\text{Li}_2\text{ZnTi}_3\text{O}_8$ was also synthesized without using $\text{Cr}(\text{NO}_3)_3$ as the raw material.

X-ray diffraction (XRD, Brook AXS's D2 PHASER) was used to examine the crystalline phase of both $\text{Li}_2\text{ZnTi}_3\text{O}_8$ and $\text{Li}_2\text{ZnTi}_{2.9}\text{Cr}_{0.1}\text{O}_8$, which was recorded within the range of $10\text{--}70^\circ$ (2θ). Scanning electron microscopy (SEM, TESCAN VEGA3) was used to examine the morphology of the samples. X-ray

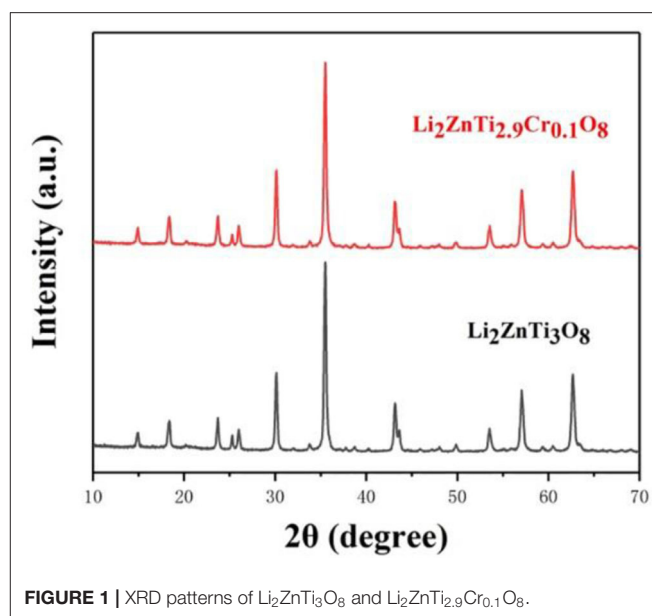


FIGURE 1 | XRD patterns of $\text{Li}_2\text{ZnTi}_3\text{O}_8$ and $\text{Li}_2\text{ZnTi}_{2.9}\text{Cr}_{0.1}\text{O}_8$.

TABLE 1 | The crystal lattice constant for $\text{Li}_2\text{ZnTi}_3\text{O}_8$ and $\text{Li}_2\text{ZnTi}_{2.9}\text{Cr}_{0.1}\text{O}_8$.

Samples	Lattice parameters	
	a(Å)	V(Å ³)
$\text{Li}_2\text{ZnTi}_{2.9}\text{Cr}_{0.1}\text{O}_8$	8.4340	599.9303
$\text{Li}_2\text{ZnTi}_3\text{O}_8$	8.4305	599.1837

photoelectron spectroscopy (XPS) with Cr-K α radiation was used to monitor the surface electronic states of the elements that were the sources of X-rays.

To construct the working electrodes, the as-prepared material, Super-P and LA-132 were mixed in weight ratios of 80:10:10 with water as solvent, and the prepared slurry was then pasted onto copper foil and dried at 100°C for 10 h in a vacuum oven. The working electrode, lithium metal, Celgard 2400 separator, and 1 M LiPF_6 electrolyte solution containing a 1:1:1 mixture of ethylene carbonate (EC), dimethyl carbonate (DMC), and ethylmethyl carbonate (EMC) were used to prepare CR2032 coin cells in an Ar-filled glovebox. All electrochemical performances were tested in the voltage range of 0.05–3.0V at room temperature.

RESULTS AND DISCUSSION

Figure 1 shows the XRD patterns of $\text{Li}_2\text{ZnTi}_3\text{O}_8$ and $\text{Li}_2\text{ZnTi}_{2.9}\text{Cr}_{0.1}\text{O}_8$. It is clear from the figure that the diffraction peaks of the samples conform to the standard diffraction peaks of cubic spinel $\text{Li}_2\text{ZnTi}_3\text{O}_8$, which demonstrates that the presence of $\text{Cr}(\text{NO}_3)_3$ does not obviously affect the structure of cubic spinel $\text{Li}_2\text{ZnTi}_3\text{O}_8$. The crystal lattice constants calculated from the recorded XRD data are listed in Table 1, and the lattice parameters of $\text{Li}_2\text{ZnTi}_3\text{O}_8$ and $\text{Li}_2\text{ZnTi}_{2.9}\text{Cr}_{0.1}\text{O}_8$ were estimated to be $a = 8.4305$ and 8.4340 \AA , respectively. The lattice

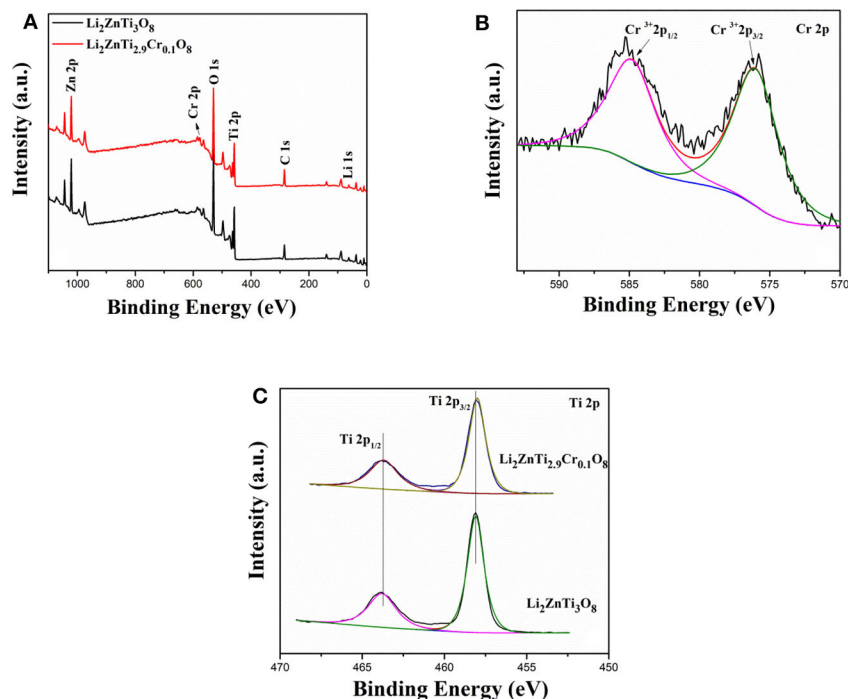


FIGURE 2 | XPS spectra of (A) XPS survey spectrum, (B) Cr 2p, (C) Ti 2p of $\text{Li}_2\text{ZnTi}_3\text{O}_8$ and $\text{Li}_2\text{ZnTi}_{2.9}\text{Cr}_{0.1}\text{O}_8$.

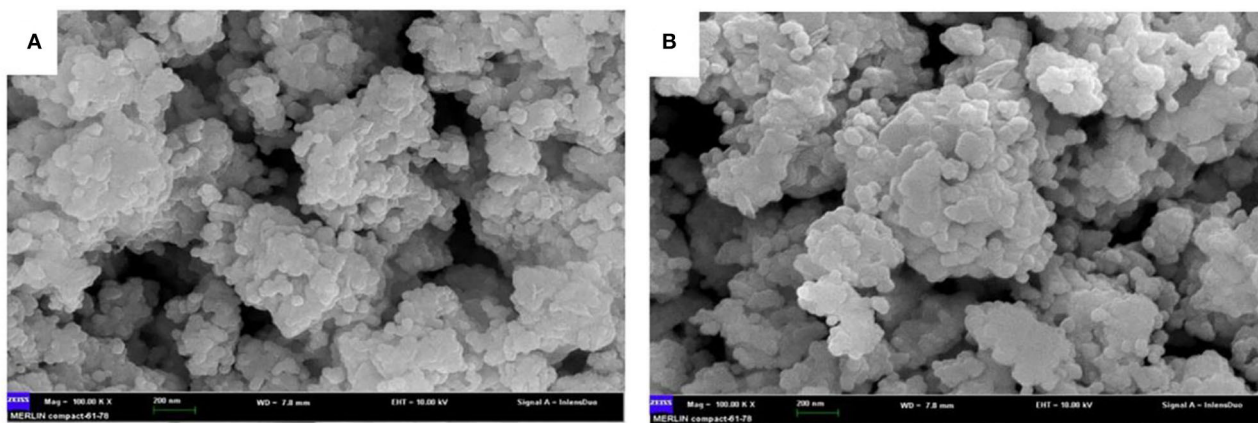


FIGURE 3 | SEM images of (A) $\text{Li}_2\text{ZnTi}_3\text{O}_8$, (B) $\text{Li}_2\text{ZnTi}_{2.9}\text{Cr}_{0.1}\text{O}_8$.

parameters increased following introduction of Cr^{3+} into the $\text{Li}_2\text{ZnTi}_3\text{O}_8$ crystal structure due to the larger radius of Cr^{3+} (0.062 nm) compared with that of Ti^{4+} (0.061 nm) (Novikova et al., 2018), which promotes the transportation of lithium ions and further enhances the electrochemical performance (Tai et al., 2020).

Additional information about the surface electronic states of the elements was gained from XPS measurements. **Figure 2A** shows the XPS survey spectra of $\text{Li}_2\text{ZnTi}_{2.9}\text{Cr}_{0.1}\text{O}_8$. As can be seen from the figure, the peaks of Li 1s, C 1s, O 1s, Ti 2p, Zn 2p, and Cr 2p are clearly visible. **Figure 2B**

reveals that two peaks centered at approximately 576.36 and 585.60 eV correspond well to the Cr $2p_{3/2}$ and Cr $2p_{1/2}$ peaks, demonstrating that Cr is present as Cr^{3+} ions in the as-synthesized $\text{Li}_2\text{ZnTi}_{2.9}\text{Cr}_{0.1}\text{O}_8$. The two peaks shown in **Figure 2C** centered at approximately 458.4 and 464.40 eV are detected for $\text{Li}_2\text{ZnTi}_3\text{O}_8$ and $\text{Li}_2\text{ZnTi}_{2.9}\text{Cr}_{0.1}\text{O}_8$, which can correspond to the peaks of Ti (IV) $2p_{3/2}$ and Ti (IV) $2p_{1/2}$.

Figure 3 shows the SEM images of the $\text{Li}_2\text{ZnTi}_3\text{O}_8$ and $\text{Li}_2\text{ZnTi}_{2.9}\text{Cr}_{0.1}\text{O}_8$ samples. It can be clearly seen that both samples are well-crystallized, with a small grain size distribution. It should be noted that the morphology of the particles did

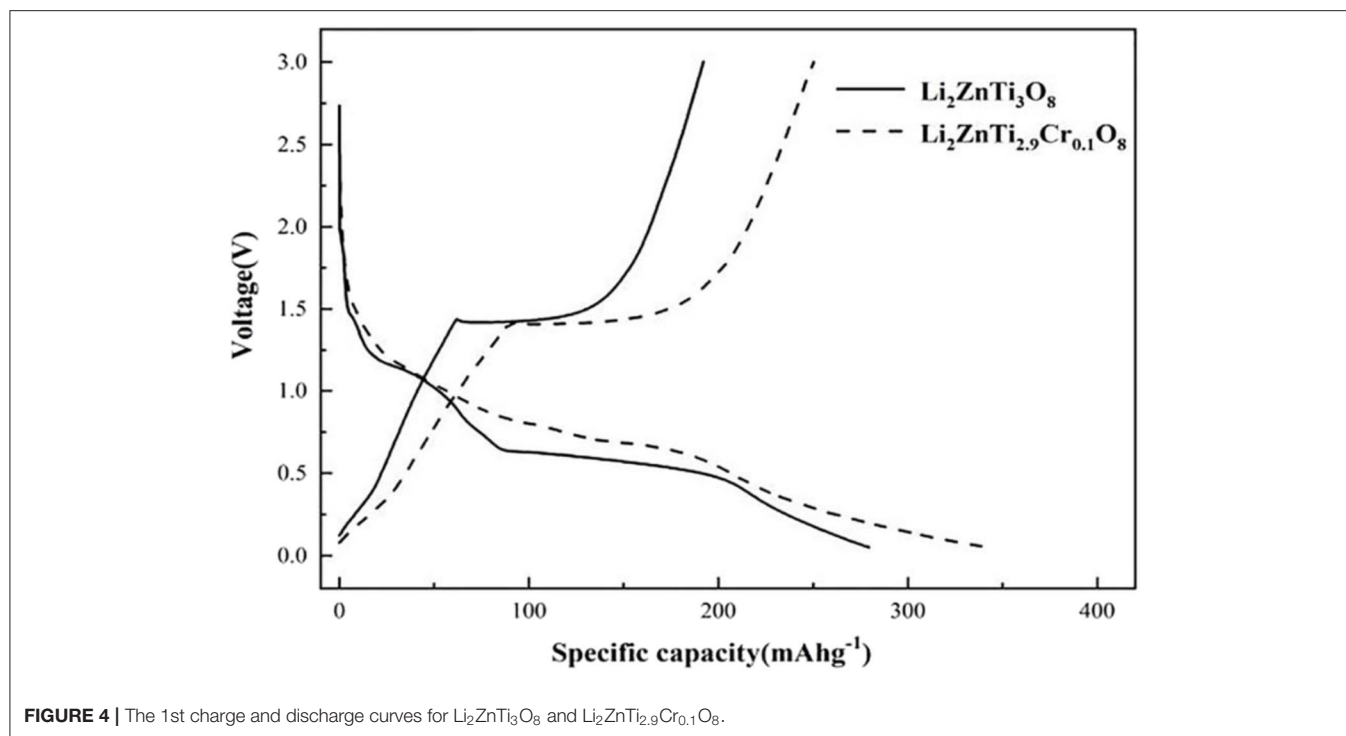


FIGURE 4 | The 1st charge and discharge curves for $\text{Li}_2\text{ZnTi}_3\text{O}_8$ and $\text{Li}_2\text{ZnTi}_{2.9}\text{Cr}_{0.1}\text{O}_8$.

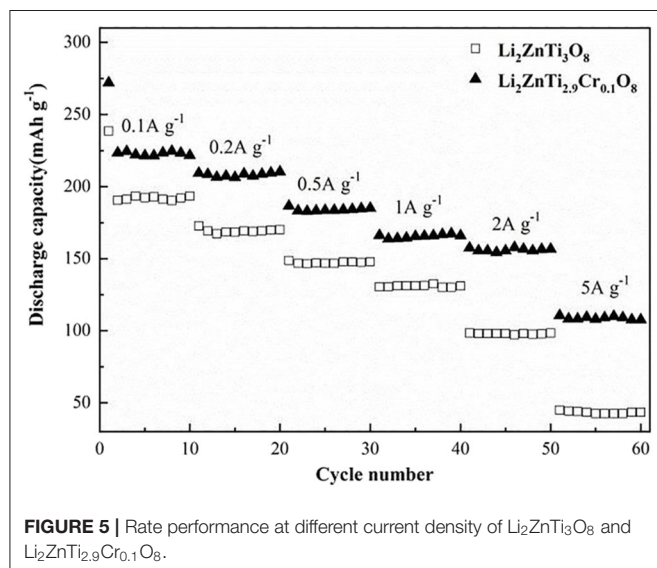


FIGURE 5 | Rate performance at different current density of $\text{Li}_2\text{ZnTi}_3\text{O}_8$ and $\text{Li}_2\text{ZnTi}_{2.9}\text{Cr}_{0.1}\text{O}_8$.

not appreciably change following doping with minute amounts of Cr^{3+} . While increasing the contact area between active particles and the electrolyte, a good dispersion can narrow the transmission distance between Li^+ and the electrons and increase the high-rate performance of 5C.

The initial charge/discharge curves of $\text{Li}_2\text{ZnTi}_3\text{O}_8$ and $\text{Li}_2\text{ZnTi}_{2.9}\text{Cr}_{0.1}\text{O}_8$ are shown in **Figure 4**, which shows that the charge/discharge curves of $\text{Li}_2\text{ZnTi}_{2.9}\text{Cr}_{0.1}\text{O}_8$ are similar to those of $\text{Li}_2\text{ZnTi}_3\text{O}_8$, suggesting that Cr^{3+} doping exerts an

effect on the electrochemical reaction. The specific capacities of $\text{Li}_2\text{ZnTi}_3\text{O}_8$ and $\text{Li}_2\text{ZnTi}_{2.9}\text{Cr}_{0.1}\text{O}_8$ at rates of 1 A g^{-1} after the first cycle were 130.5 and $166.8 \text{ mA h g}^{-1}$, respectively. As can clearly be seen, $\text{Li}_2\text{ZnTi}_{2.9}\text{Cr}_{0.1}\text{O}_8$ demonstrates a higher specific capacity than $\text{Li}_2\text{ZnTi}_3\text{O}_8$. This can be explained by the fact that Cr doping can enlarge the transport tunnel of lithium ions, which further increases lithium ion transportation and electron transfer, thus enhancing the electronic conductivity (Zhang et al., 2018). In addition, $\text{Li}_2\text{ZnTi}_{2.9}\text{Cr}_{0.1}\text{O}_8$ appears to have the least voltage platform difference, indicating that a lower electrode polarization was obtained following Cr^{3+} doping and Li^+ transport was improved.

The rate performances of $\text{Li}_2\text{ZnTi}_3\text{O}_8$ and $\text{Li}_2\text{ZnTi}_{2.9}\text{Cr}_{0.1}\text{O}_8$ are compared in **Figure 5**. $\text{Li}_2\text{ZnTi}_{2.9}\text{Cr}_{0.1}\text{O}_8$ delivered maximum discharge capacities of 221.7, 210.3, 185.1, 166, 156.7, and $107.5 \text{ mA h g}^{-1}$ at 0.1, 0.2, 0.5, 1, 2, and 5 C, respectively, whereas $\text{Li}_2\text{ZnTi}_3\text{O}_8$ delivered 193.4, 170.2, 147.8, 131, 98.3, and 43.5 mA h g^{-1} at the same rates, respectively. As can be seen, $\text{Li}_2\text{ZnTi}_{2.9}\text{Cr}_{0.1}\text{O}_8$ showed better rate performance compared with $\text{Li}_2\text{ZnTi}_3\text{O}_8$, which may be due to either or both of the following reasons: (1) Cr doping improves the electronic conductivity, which leads to $\text{Li}_2\text{ZnTi}_{2.9}\text{Cr}_{0.1}\text{O}_8$ demonstrating better electrochemical performance than $\text{Li}_2\text{ZnTi}_3\text{O}_8$; (2) the improved cell volume following Cr doping enhances lithium ion diffusion and electron transfer (Chen et al., 2009; Nie et al., 2020).

The cycling performance of $\text{Li}_2\text{ZnTi}_3\text{O}_8$ and $\text{Li}_2\text{ZnTi}_{2.9}\text{Cr}_{0.1}\text{O}_8$ was examined at a rate of 1 A g^{-1} , and the results are shown in **Figure 6**. As seen, the coulombic efficiency of $\text{Li}_2\text{ZnTi}_3\text{O}_8$ and $\text{Li}_2\text{ZnTi}_{2.9}\text{Cr}_{0.1}\text{O}_8$ were 80.2 and 84.8% in

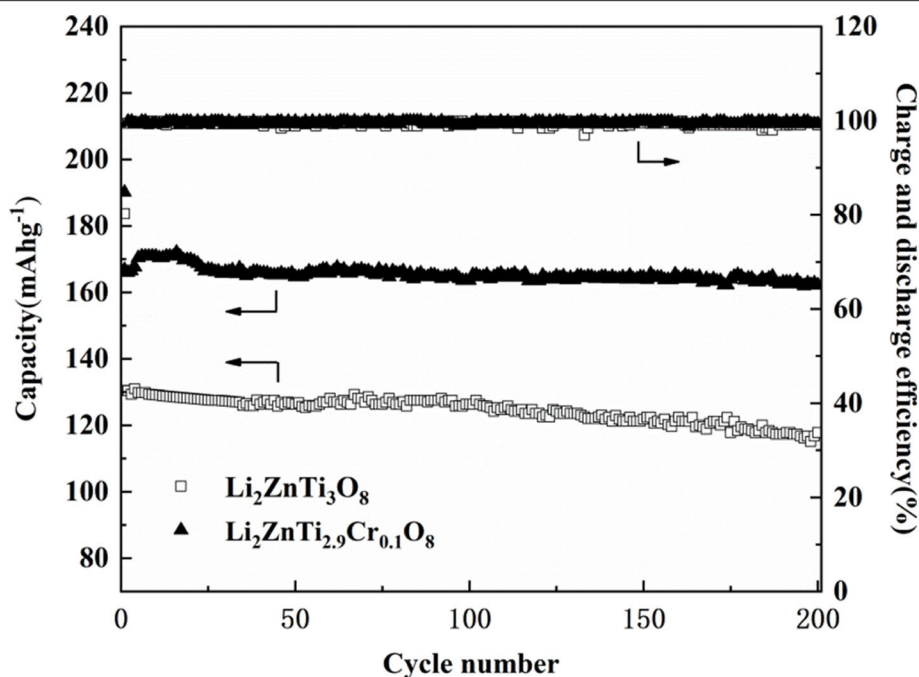


FIGURE 6 | Cycling capacity of $\text{Li}_2\text{ZnTi}_3\text{O}_8$ and $\text{Li}_2\text{ZnTi}_{2.9}\text{Cr}_{0.1}\text{O}_8$ for 200 cycles.

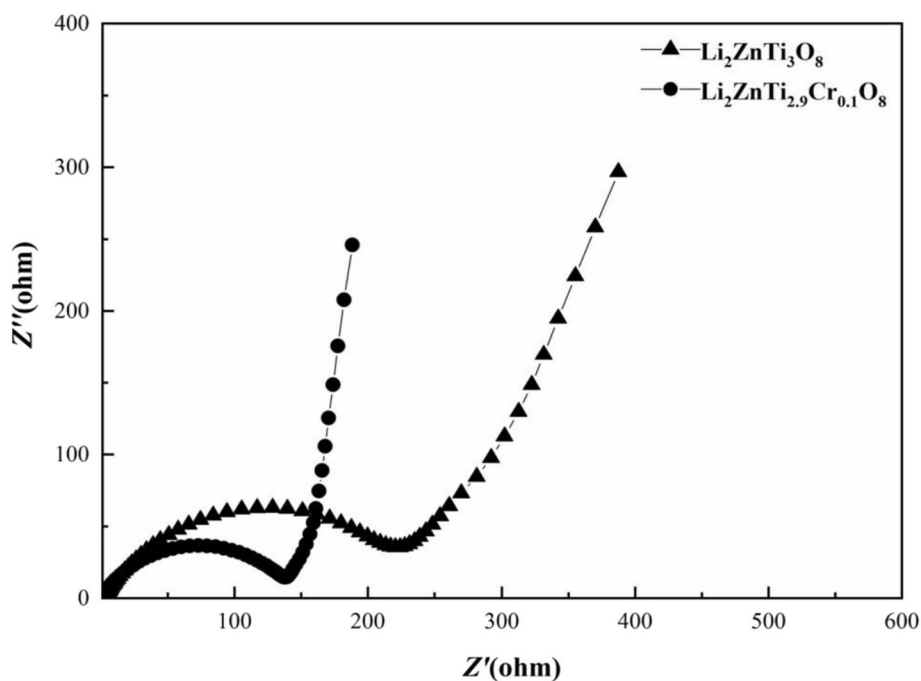


FIGURE 7 | EIS of pure $\text{Li}_2\text{ZnTi}_3\text{O}_8$ and $\text{Li}_2\text{ZnTi}_{2.9}\text{Cr}_{0.1}\text{O}_8$.

the first cycle, indicating that the coulombic efficiency can be enhanced after Cr doped. After several cycles, the coulombic efficiency of two samples is close to 100%. After 200 cycles, the reserving ratios were 90.2 and 97.2% for $\text{Li}_2\text{ZnTi}_3\text{O}_8$ and

$\text{Li}_2\text{ZnTi}_{2.9}\text{Cr}_{0.1}\text{O}_8$, respectively. Therefore, $\text{Li}_2\text{ZnTi}_{2.9}\text{Cr}_{0.1}\text{O}_8$ possesses the better cycling performance. These results indicate that $\text{Li}_2\text{ZnTi}_{2.9}\text{Cr}_{0.1}\text{O}_8$ shows better capacity retention than $\text{Li}_2\text{ZnTi}_3\text{O}_8$, which can probably be explained by assuming that

moderate Cr doping can enlarge the transport tunnel of lithium ions, which further increases lithium ion transportation and electron transfer.

Electrochemical impedance spectroscopy (EIS) measurements for $\text{Li}_2\text{ZnTi}_3\text{O}_8$ and $\text{Li}_2\text{ZnTi}_{2.9}\text{Cr}_{0.1}\text{O}_8$ were carried out to probe the kinetic properties of these anode materials, and the results are shown in **Figure 7**. Similar patterns are displayed by the impedance spectra of the two samples, which formed a semicircle in the high-frequency regions and a straight line in the low-frequency regions. The semicircle in the high-frequency regions is associated with charge transfer resistance on the electrode/electrolyte interface, while the straight line in the low-frequency regions is ascribed to the diffusion of Li^+ into the Warburg resistance (Long et al., 2011; Tang et al., 2019), which constitutes the bulk of the electrode materials. It is clear that the charge transfer resistance of the $\text{Li}_2\text{ZnTi}_{2.9}\text{Cr}_{0.1}\text{O}_8$ electrode material is lower than that of $\text{Li}_2\text{ZnTi}_3\text{O}_8$, showing that a certain small amount of Cr^{3+} doping of $\text{Li}_2\text{ZnTi}_3\text{O}_8$ is useful for enhancing the electronic conductivity (Li Z. F. et al., 2016; Kou et al., 2020). In addition, the slope for the $\text{Li}_2\text{ZnTi}_{2.9}\text{Cr}_{0.1}\text{O}_8$ electrode material in the low-frequency regions is slightly higher than that for $\text{Li}_2\text{ZnTi}_3\text{O}_8$ because Cr doping can strengthen lithium ion migration through $\text{Li}_2\text{ZnTi}_3\text{O}_8$.

CONCLUSIONS

This study successfully prepared $\text{Li}_2\text{ZnTi}_3\text{O}_8$ and $\text{Li}_2\text{ZnTi}_{2.9}\text{Cr}_{0.1}\text{O}_8$ samples with the cubic spinel structure by the sol-gel method. XRD revealed that the element Cr

successfully doped into the $\text{Li}_2\text{ZnTi}_3\text{O}_8$ exerted no effect on the spinel structure of $\text{Li}_2\text{ZnTi}_3\text{O}_8$. SEM (Chen B. K. et al., 2015) results demonstrated that the morphology of the particles did not obviously change following Cr^{3+} doping. The measured electrochemical properties indicated that $\text{Li}_2\text{ZnTi}_{2.9}\text{Cr}_{0.1}\text{O}_8$ shows a better rate performance and excellent cyclic reversibility than $\text{Li}_2\text{ZnTi}_3\text{O}_8$. The electrochemical performance might be significantly enhanced as a result of the higher electronic conductivity following Cr^{3+} doping, demonstrating that $\text{Li}_2\text{ZnTi}_{2.9}\text{Cr}_{0.1}\text{O}_8$ is a promising anode material for high-rate LIBs.

DATA AVAILABILITY STATEMENT

All datasets presented in this study are included in the article/supplementary material.

AUTHOR CONTRIBUTIONS

XZ and JP contributed conception and design of the study. HZ and YG organized the database. JP and XH wrote the first draft of the manuscript. XZ revised the whole manuscript. All authors contributed to the article and approved the submitted version.

FUNDING

This work was financially supported by Key Projects of Zigong Science and Technology Bureau (2018CXJD07).

REFERENCES

- An, F. Q., Zhao, H. L., Cheng, Z., Qiu, J. Y. C., Zhou, W. N., and Li, P. (2019). Development status and research progress of power battery for pure electric vehicles. *Chin. J. Eng.* 1, 22–42. doi: 10.13374/j.issn2095-9389.2019.01.003
- Bai, Y. J., Gong, C., Qi, Y. X., Lun, N., and Feng, J. (2012). Excellent long-term cycling stability of La-doped $\text{Li}_4\text{Ti}_5\text{O}_{12}$ anode material at high current rate. *J. Mater. Chem.* 22, 19054–19060. doi: 10.1039/c2jm34523d
- Chen, B. K., Du, C. J., Zhang, Y. Z., Sun, R. X., Zhou, L., and Wang, L. J. (2015). A new strategy for synthesis of lithium zinc titanate as an anode material for lithium ion batteries. *Electrochim. Acta* 159, 102–110. doi: 10.1016/j.electacta.2015.01.206
- Chen, C., Ai, C. C., and Liu, X. Y. (2018). Ti(III) self-doped $\text{Li}_2\text{ZnTi}_3\text{O}_8$ as a superior anode material for Li-ion batteries. *Electrochim. Acta* 265, 448–454. doi: 10.1016/j.electacta.2018.01.159
- Chen, W., Zhou, Z. R., Wang, R. R., Wu, Z. T., Liang, H. F., Shao, L. Y., et al. (2015). High performance Na-doped lithium zinc titanate as anode material for Li-ion batteries. *RSC Adv.* 5, 49890–49898. doi: 10.1039/C5RA06365E
- Chen, Y. H., Zhao, Y. M., An, X. N., Liu, J. M., Dong, Y. Z., and Chen, L. (2009). Preparation and electrochemical performance studies on Cr-doped $\text{Li}_3\text{V}_2(\text{PO}_4)_3$ as cathode materials for lithium-ion batteries. *Electrochim. Acta* 54, 5844–5850. doi: 10.1016/j.electacta.2009.05.041
- Dong-il, R., and Han, K. S. (2006). Used lithium ion rechargeable battery recycling using Etoile-Rebatt technology. *J. Power Sources* 163, 284–288. doi: 10.1016/j.jpowsour.2006.05.040
- Fang, W., Cheng, X. Q., Zuo, P. J., Ma, Y. L., and Yin, G. P. (2013). A facile strategy to prepare nano-crystalline $\text{Li}_4\text{Ti}_5\text{O}_{12}/\text{C}$ anode material via polyvinyl alcohol as carbon source for high-rate rechargeable Li-ion batteries. *Electrochim. Acta* 93, 173–178. doi: 10.1016/j.electacta.2013.01.112
- Feng, Y., Li, Y. L., and Hou, F. (2009). Preparation and electrochemical properties of Cr doped LiV_3O_8 cathode for lithium ion batteries. *Mater. Lett.* 63, 1338–1340. doi: 10.1016/j.matlet.2009.03.009
- Hong, X. D., Huang, X. B., Ren, Y. R., Wang, H. Y., Ding, X., and Jin, J. L. (2019). Superior Na-storage performance of $\text{Na}_3\text{V}_2(\text{PO}_4)_3/\text{C}$ -Ag composites as cathode material for Na-ion battery. *J. Alloys Compd.* 822:153587. doi: 10.1016/j.jallcom.2019.153587
- Huang, X. B., Yin, X., Yang, Q., Guo, Z. H., Ren, Y. R., and Zeng, X. G. (2020). Outstanding electrochemical performance of N/S co-doped carbon/ $\text{Na}_3\text{V}_2(\text{PO}_4)_3$ hybrid as the cathode of a sodium-ion battery. *Ceramics Int.* 46, 28084–28090. doi: 10.1016/j.ceramint.2020.07.303
- Jhan, Y. R., and Duh, J. G. (2012). Electrochemical performance and low discharge cut-off voltage behavior of ruthenium doped $\text{Li}_4\text{Ti}_5\text{O}_{12}$ with improved energy density. *Electrochim. Acta* 63, 9–15. doi: 10.1016/j.electacta.2011.12.014
- Jović, N., Vučinić-Vasić, M., Kremenović, A., Antić, B., Jovalekić, C., Vulić, P., et al. (2009). HEBM synthesis of nanocrystalline $\text{LiZn}_{0.5}\text{Ti}_{1.5}\text{O}_4$ spinel and thermally induced order-disorder phase transition. *Mater. Chem. Phys.* 116, 542–549. doi: 10.1016/j.matchemphys.2009.04.033
- Junmin, N., Han, D., and Zuo, X. (2005). Recovery of metal values from spent lithium-ion batteries with chemical deposition and solvent extraction. *J. Power Sources* 152, 278–284. doi: 10.1016/j.jpowsour.2005.03.134
- Kou, Z. Y., Miao, C., Mei, P., Zhang, Y., Yan, X. M., Jiang, Y., et al. (2020). Enhancing the cycling stability of all-solid-state lithium-ion batteries assembled with $\text{Li}_{1.3}\text{Al}_{0.3}\text{Ti}_{1.7}(\text{PO}_4)_3$ solid electrolytes prepared from precursor solutions with appropriate pH values. *Ceramics Int.* 46, 9629–9636. doi: 10.1016/j.ceramint.2019.12.229
- Lee, J. S., Wang, X. Q., Luo, H. M., and Dai, S. (2010). Fluidic carbon precursors for formation of functional carbon under ambient pressure based on ionic liquids. *Adv. Mater.* 22, 1004–1007. doi: 10.1002/adma.200903403
- Li, G. H., Li, F. C., Yang, H., Cheng, F. Y., Xu, N., Shi, W., et al. (2016). Graphene oxides doped MIL-101(Cr) as anode materials for enhanced electrochemistry

- performance of lithium ion battery. *Inorg. Chem. Commun.* 64, 63–66. doi: 10.1016/j.inoche.2015.12.017
- Li, Z. F., Cui, Y. H., Wu, J. W., Du, C. Q., Zhang, X. H., and Tang, Z. Y. (2016). Synthesis and electrochemical properties of lithium zinc titanate as an anode material for lithium ion batteries via microwave method. *RSC Adv.* 45, 39209–39215. doi: 10.1039/C6RA05244D
- Lin, C. F., Lai, M. O., Zhou, H. H., and Lu, L. (2014). Mesoporous $\text{Li}_4\text{Ti}_5\text{O}_{12-x}/\text{C}$ submicrospheres with comprehensively improved electrochemical performances for high-power lithium-ion batteries. *Phys. Chem. Chem. Phys.* 16, 24874–24883. doi: 10.1039/C4CP03826F
- Lin, J. Y., Hsu, C. C., Ho, H. P., and Wu, S. H. (2013). Sol-gel synthesis of aluminum doped lithium titanate anode material for lithium ion batteries. *Electrochim. Acta* 87, 126–132. doi: 10.1016/j.electacta.2012.08.128
- Lin, Y., Jhan, Y. R., and Duh, J. G. (2011). Improved capacity and rate capability of Ru-doped and carbon-coated $\text{Li}_4\text{Ti}_5\text{O}_{12}$ anode material. *J. Alloys Compd.* 509, 6965–6968. doi: 10.1016/j.jallcom.2011.04.018
- Liu, M., Wang, X. Y., Wei, S. Y., Hu, H., Zhang, R., and Liu, L. (2018). Cr-doped $\text{Fe}_2\text{F}_5\text{-H}_2\text{O}$ with open framework structure as a high performance cathode material of sodium-ion batteries. *Electrochim. Acta* 269, 479–489. doi: 10.1016/j.electacta.2018.02.159
- Liu, T., Tang, H. Q., Zan, L. X., and Tang, Z. Y. (2016). Comparative study of $\text{Li}_2\text{ZnTi}_3\text{O}_8$ anode material with good high rate capacities prepared by solid state, molten salt and sol-gel methods. *J. Electroanal. Chem.* 771, 10–16. doi: 10.1016/j.jelechem.2016.03.036
- Long, W. M., Wang, X. Y., Yang, S. Y., Shu, H. B., Wu, Q., Bai, Y. S., et al. (2011). Electrochemical properties of $\text{Li}_4\text{Ti}_5-2x\text{Ni}_x\text{Mn}_x\text{O}_{12}$ compounds synthesized by sol-gel process. *Mater. Chem. Phys.* 131, 431–435. doi: 10.1016/j.matchemphys.2011.09.071
- Mani, V., Nathiya, K., and Kalaiselvi, N. (2014). Role of carbon content in qualifying $\text{Li}_3\text{V}_2(\text{PO}_4)_3/\text{C}$ as a high capacity anode for high rate lithium battery applications. *RSC Adv.* 4, 17091–17096. doi: 10.1039/C4RA00963K
- Nie, Y., Xiao, W., Miao, C., Fang, R., Kou, Z. Y., Wang, D., et al. (2020). Boosting the electrochemical performance of $\text{LiNi}_{0.8}\text{Co}_{0.15}\text{Al}_{0.05}\text{O}_2$ cathode materials *in-situ* modified with $\text{Li}_{1.3}\text{Al}_{0.3}\text{Ti}_{1.7}(\text{PO}_4)_3$ fast ion conductor for lithium-ion batteries. *Electrochim. Acta* 353:136477. doi: 10.1016/j.electacta.2020.136477
- Novikova, S. A., Larkovich, R. V., Chekannikov, A. A., Kulova, T. L., and Yaroslavtsev, A. B. (2018). Electrical conductivity and electrochemical characteristics of $\text{Na}_3\text{V}_2(\text{PO}_4)_3$ -based NASICON-type materials. *Inorg. Mater.* 54, 794–804. doi: 10.1134/S0020168518080149
- Pan, X., Duan, X. C., Lin, X. P., Zong, F. Y., Tong, X. B., Li, Q. H., et al. (2018). Rapid synthesis of Cr-doped gamma- Fe_2O_3 /reduced graphene oxide nanocomposites as high performance anode materials for lithium ion batteries. *J. Alloys Compd.* 732, 270–279. doi: 10.1016/j.jallcom.2017.10.222
- Qi, Y. L., Huang, Y. D., Jia, D. Z., Bao, S. J., and Guo, Z. P. (2009). Preparation and characterization of novel spinel $\text{Li}_4\text{Ti}_5\text{O}_{12-x}\text{Br}_x$ anode materials. *Electrochim. Acta* 54, 4772–4776. doi: 10.1016/j.electacta.2009.04.010
- Ruan, Y. L., Wang, K., Song, S. D., Liu, J. J., and Han, X. (2017). Improved structural stability and electrochemical performance of $\text{Na}_3\text{V}_2(\text{PO}_4)_3$ cathode material by Cr doping. *Ionics* 23, 1097–1105. doi: 10.1007/s11581-016-1919-3
- Shenouda, Y., and Murali, K. R. (2008). Electrochemical properties of doped lithium titanate compounds and their performance in lithium rechargeable batteries. *J. Power Sources* 176, 332–339. doi: 10.1016/j.jpowsour.2007.10.061
- Tai, Z. G., Zhu, W., Shi, M., Xin, Y. F., Guo, S. W., Wu, Y. F., et al. (2020). Improving electrochemical performances of Lithium-rich oxide by cooperatively doping Cr and coating Li_3PO_4 as cathode material for Lithium-ion batteries. *J. Colloid Interface Sci.* 576, 468–475. doi: 10.1016/j.jcis.2020.05.015
- Tang, H. Q., and Tang, Z. Y. (2014). Effect of different carbon sources on electrochemical properties of $\text{Li}_2\text{ZnTi}_3\text{O}_8/\text{C}$ anode material in lithium-ion batteries. *J. Alloys Compd.* 613, 267–274. doi: 10.1016/j.jallcom.2014.06.050
- Tang, H. Q., Tang, Z. Y., Du, C. Q., Qie, F. C., and Zhu, J. T. (2014a). Ag-doped $\text{Li}_2\text{ZnTi}_3\text{O}_8$ as a high rate anode material for rechargeable lithium-ion batteries. *Electrochim. Acta* 120, 187–192. doi: 10.1016/j.electacta.2013.12.090
- Tang, H. Q., Zhu, J. T., Tang, Z. Y., and Ma, C. X. (2014b). Al-doped $\text{Li}_2\text{ZnTi}_3\text{O}_8$ as an effective anode material for lithium-ion batteries with good rate capabilities. *J. Electroanal. Chem.* 731, 60–65. doi: 10.1016/j.jelechem.2014.08.011
- Tang, Y. Q., Liu, L., Huang, X. B., Ding, X., Zhou, S. B., and Chen, Y. D. (2019). Synthesis and electrochemical properties of $\text{Li}_2\text{FeSiO}_4/\text{C}/\text{Ag}$ composite as a cathode material for Li-ion battery. *J. Central South Univ.* 26, 1443–1448. doi: 10.1007/s11771-019-4100-0
- Tarascon, J. M., and Armand, M. (2001). Issues and challenges facing rechargeable lithium batteries. *Nature* 414, 359–367. doi: 10.1038/35104644
- Tian, B. B., Xiang, H. F., Zhang, L., Li, Z., and Wang, H. H. (2010). Niobium doped lithium titanate as a high rate anode material for Li-ion batteries. *Electrochim. Acta* 55, 5453–5458. doi: 10.1016/j.electacta.2010.04.068
- Wang, M. X., Huang, X. B., Wang, H. Y., Zhou, T., Xie, H. S., and Ren, Y. R. (2019). Synthesis and electrochemical performances of $\text{Na}_3\text{V}_2(\text{PO}_4)_2\text{F}_3/\text{C}$ composites as cathode materials for sodium ion batteries. *RSC Adv.* 9, 30628–30636. doi: 10.1039/C9RA05089B
- Wang, M. X., Wang, K., Huang, X. B., Zhou, T., Xie, H. S., and Ren, Y. R. (2020). Improved sodium storage properties of Zr-doped $\text{Na}_3\text{V}_2(\text{PO}_4)_2\text{F}_3/\text{C}$ as cathode material for sodium ion batteries. *Ceramics Int.* 46, 28490–28498. doi: 10.1016/j.ceramint.2020.08.006
- Wang, S., Bi, Y. F., Wang, L. J., Meng, Z. H., and Luo, B. M. (2019). Mo-doped $\text{Li}_2\text{ZnTi}_3\text{O}_8$ at graphene as a high performance anode material for lithium-ion batteries. *Electrochim. Acta* 301, 319–324. doi: 10.1016/j.electacta.2019.01.168
- Wu, H. B., Chang, S., Liu, X. L., Yu, L. Q., Wang, G. L., Cao, D. X., et al. (2013). Sr-doped $\text{Li}_4\text{Ti}_5\text{O}_{12}$ as the anode material for lithium-ion batteries. *Solid State Ionics* 232, 13–18. doi: 10.1016/j.ssi.2012.10.027
- Xiao, H., Huang, X. B., Ren, Y. R., Ding, X., Chen, Y. D., and Zhou, S. B. (2019). Improved electrochemical performance of $\text{Na}_3\text{V}_2(\text{PO}_4)_3$ modified by N-doped carbon coating and Zr doping. *Solid State Ionics* 333, 93–100. doi: 10.1016/j.ssi.2019.01.025
- Xiao, H., Huang, X. B., Ren, Y. R., Wang, H. Y., Ding, J. N., Zhou, S. B., et al. (2018). Enhanced sodium ion storage performance of $\text{Na}_3\text{V}_2(\text{PO}_4)_3$ with N-doped carbon by folic acid as carbon-nitrogen source. *J. Alloys Compd.* 732, 454–459. doi: 10.1016/j.jallcom.2017.10.195
- Xu, Y. X., Hong, Z. S., Xia, L. C., Yang, J., and Wei, M. D. (2013). One step sol-gel synthesis of $\text{Li}_2\text{ZnTi}_3\text{O}_8/\text{C}$ nanocomposite with enhanced lithium-ion storage properties. *Electrochim. Acta* 88, 74–78. doi: 10.1016/j.electacta.2012.10.044
- Yi, T. F., Pan, J. J., Wei, T. T., Li, Y. W., and Cao, G. Z. (2020a). NiCo_2S_4 -based nanocomposites for energy storage in supercapacitors and batteries. *Nano Today* 33:100894. doi: 10.1016/j.nantod.2020.100894
- Yi, T. F., Qiu, L. Y., Mei, J., Qi, S. Y., Cui, P., Luo, S. H., et al. (2020c). Porous spherical $\text{NiO}/\text{NiMoO}_4/\text{PPy}$ nanoarchitectures as advanced electrochemical pseudocapacitor materials. *Sci. Bull.* 65, 546–556. doi: 10.1016/j.scib.2020.01.011
- Yi, T. F., Wei, T. T., Li, Y., He, Y. B., and Wang, Z. B. (2020b). Efforts on enhancing the Li-ion diffusion coefficient and electronic conductivity of titanate-based anode materials for advanced Li-ion batteries. *Energy Stor. Mater.* 26, 165–197. doi: 10.1016/j.ensm.2019.12.042
- Yoshio, N. (2001). Lithium ion secondary batteries; past 10 years and the future. *J. Power Sources* 100, 101–106. doi: 10.1016/S0378-7753(01)00887-4
- Yu, Z. J., Zhang, X. F., Yang, G. L., Liu, J., Wang, J. W., Wang, R. S., et al. (2011). High rate capability and long-term cyclability of $\text{Li}_4\text{Ti}_4.9\text{V}_{0.1}\text{O}_{12}$ as anode material in lithium ion battery. *Electrochim. Acta* 56, 8611–8617. doi: 10.1016/j.electacta.2011.07.051
- Zhang, B., Huang, Z. D., Oh, S. W., and Kim, J. K. (2011). Improved rate capability of carbon coated $\text{Li}_{3.9}\text{Sn}_{0.1}\text{Ti}_5\text{O}_{12}$ porous electrodes for Li-ion batteries. *J. Power Sources* 196, 10692–10697. doi: 10.1016/j.jpowsour.2011.08.114
- Zhang, P., Li, X. L., Hua, Y., Yu, J. J., S., and Ding, Y. (2018). Enhanced performance and anchoring polysulfide mechanism of carbon aerogel/sulfur material with Cr doping and pore tuning for Li-S batteries. *Electrochim. Acta* 282, 499–509. doi: 10.1016/j.electacta.2018.06.068

Conflict of Interest: HZ was employed by the company Langxingda Technology Co, Ltd.

The remaining authors declare that the research was conducted in the absence of any commercial or financial relationships that could be construed as a potential conflict of interest.

Copyright © 2021 Zeng, Peng, Zhu, Gong and Huang. This is an open-access article distributed under the terms of the Creative Commons Attribution License (CC BY). The use, distribution or reproduction in other forums is permitted, provided the original author(s) and the copyright owner(s) are credited and that the original publication in this journal is cited, in accordance with accepted academic practice. No use, distribution or reproduction is permitted which does not comply with these terms.